Biochemical and Biophysical Research Communications 444 (2014) 92–97

Contents lists available at ScienceDirect

Biochemical and Biophysical Research Communications

journal homepage: www.elsevier.com/locate/ybbrc

Effect of amino acid variations in the central region of human serum amyloid A on the amyloidogenic properties

Hiroka Takase [a], Masafumi Tanaka [a,*], Sachiko Miyagawa [a], Toshiyuki Yamada [b], Takahiro Mukai [a]

[a] Department of Biophysical Chemistry, Kobe Pharmaceutical University, Kobe 658-8558, Japan
[b] Department of Clinical Laboratory Medicine, Jichi Medical University, Shimotsuke 329-0498, Japan

ARTICLE INFO

Article history:
Received 27 December 2013
Available online 16 January 2014

Keywords:
Amino acid variation
Amyloid fibril formation
Fibril morphology
Serum amyloid A
Synthetic fragment peptide

ABSTRACT

Human serum amyloid A (SAA) is a precursor protein of the amyloid fibrils that are responsible for AA amyloidosis. Of the four human SAA genotypes, SAA1 is most commonly associated with AA amyloidosis. Furthermore, SAA1 has three major isoforms (SAA1.1, 1.3, and 1.5) that differ by single amino acid variations at two sites in their 104-amino acid sequences. In the present study, we examined the effect of amino acid variations in human SAA1 isoforms on the amyloidogenic properties. All SAA1 isoforms adopted α-helix structures at 4 °C, but were unstructured at 37 °C. Heparin-induced amyloid fibril formation of SAA1 was observed at 37 °C, as evidenced by the increased thioflavin T (ThT) fluorescence and β-sheet structure formation. Despite a comparable increase in ThT fluorescence, SAA1 molecules retained their α-helix structures at 4 °C. At both temperatures, no essential differences in ThT fluorescence and secondary structures were observed among the SAA1 isoforms. However, the fibril morphologies appeared to differ; SAA1.1 formed long and curly fibrils, whereas SAA1.3 formed thin and straight fibrils. The peptides corresponding to the central regions of the SAA1 isoforms containing amino acid variations showed distinct amyloidogenicities, reflecting their direct effects on amyloid fibril formation. These findings may provide novel insights into the influence of amino acid variations in human SAA on the pathogenesis of AA amyloidosis.

1. Introduction

Human serum amyloid A (SAA) is a precursor protein of AA amyloidosis, which is among the most severe complications that occur secondary to chronic inflammatory diseases such as rheumatoid arthritis [1]. Although persistently high concentrations of SAA proteins comprise a plausible risk factor for AA amyloidosis, a detailed molecular mechanism has not been elucidated. AA amyloidosis occurs in only 5–10% of humans during persistent chronic inflammatory conditions [2], indicating the existence of disease-modifying factors [3]. Instead of full-length SAA proteins (104 amino acids), the N-terminal fragments mainly consisting of 76-amino acid SAA molecules known as AA fragments have been detected in amyloid deposits [4]. Although several enzymes are known to be involved in SAA degradation, it has not been revealed whether enzymatic SAA cleavage is an essential prerequisite for amyloid deposition in AA amyloidosis. In addition, because heparan sulfate proteoglycan has been found in amyloid deposits, glycosaminoglycans are presumed to facilitate amyloid fibril formation as a scaffold for protein aggregation [5]. These biomolecules can act as disease-modifying factors through a currently unknown mechanism.

At least 20 different amyloid-forming proteins have been identified and associated with human diseases, including amyloid-β peptide with Alzheimer's disease and α-synuclein with Parkinson's disease [6]. Amyloid fibrils formed by these different proteins share some common structural features [7]. For example, amyloid fibrils are typically straight, with unbranched morphology. Another feature is a β-sheet secondary protein structure, in which β-strands run perpendicular to the fibril axis. Fluorescent dyes such as Congo red and thioflavin T (ThT), which bind to β-sheet structures, are used to indicate fibril formation. In some cases, the ThT emission intensity selectively increases by several orders in the presence of amyloid fibrils [8]. These characteristics allow us to determine amyloid fibril formation and are employed as common experimental techniques in amyloid research.

There are four human SAA genes (*SAA1–4*), of which *SAA3* is a pseudogene. SAA1 and SAA2 are synthesized during acute-phase inflammatory reactions, whereas SAA4 is a constitutively

Abbreviations: CD, circular dichroism; SAA, serum amyloid A; ThT, thioflavin T; TEM, transmission electron microscopy.

* Corresponding author. Address: Department of Biophysical Chemistry, Kobe Pharmaceutical University, 4-19-1 Motoyamakita-machi, Higashinada-ku, Kobe 658-8558, Japan. Fax: +81 78 441 7541.
E-mail address: masatnk@kobepharma-u.ac.jp (M. Tanaka).

0006-291X/$ - see front matter © 2014 Elsevier Inc. All rights reserved.
http://dx.doi.org/10.1016/j.bbrc.2014.01.029

expressed protein. SAA1 and SAA2 are allelic, giving rise to three distinct SAA1 isoforms (SAA1.1, 1.3, and 1.5) and two SAA2 isoforms (SAA2.1 and SAA2.2). SAA1 is most commonly associated with AA amyloidosis, probably because the circulating concentration of SAA1 is much higher than that of SAA2. The SAA1 isoforms differ by single amino acid variations at two sites, which are considered to affect the susceptibility to AA amyloidosis [9]. Thus, it is conceivable that the SAA1 isoforms could be disease-modifying factors. However, currently there is no direct molecular evidence to demonstrate that amino acid variations in the SAA1 isoforms affect fibril formation.

Using synthetic fragment peptides, we previously revealed that not only the N-terminal region but also the central region of the SAA molecule is involved in amyloid fibril formation [10]. The central region of SAA1 contains the isoform-associated amino acid variations, specifically SAA1.1 (52Val, 57Ala), SAA1.3 (52Ala, 57Ala), and SAA1.5 (52Ala, 57Val). Thus, in the present study, the effects of amino acid variations on the SAA molecule fibril formation were investigated using full-length SAA1 proteins that contain the amyloidogenic N-terminal region common to the three SAA1 isoforms as well as fragment peptides derived from the central regions of the SAA1 isoforms.

2. Materials and methods

2.1. Materials

Heparin sodium and ThT were purchased from Celsus Laboratories (Cincinnati, OH) and Sigma–Aldrich (St. Louis, MO), respectively. Fmoc amino acid derivatives were obtained from the Peptide Institute, Inc. (Minoh, Japan) and used without further purification. The buffers used were 10 mM sodium phosphate (pH 7.4), 10 mM sodium citrate (pH 5.6), or 10 mM sodium acetate (pH 4.0). All other reagents were special or peptide synthesis grade.

2.2. Preparation of SAA proteins and peptides

The recombinant human SAA1 isoforms SAA1.1 (52Val, 57Ala), SAA1.3 (52Ala, 57Ala), and SAA1.5 (52Ala, 57Val) were produced in *Escherichia coli*. Each plasmid corresponding to an SAA1 isotype was constructed and transformed into *E. coli* BL21 cells as previously described [11]. Recombinant proteins were prepared from expression-induced *E. coli* lysates according to the methods described [12]; these proteins contained an extra Met residue at the N-terminus.

The primary sequences of the synthetic fragment peptides used in the present study are listed in Table 1. Peptide synthesis and purification were performed according to the methods described [13]. Peptides were synthesized by the solid-phase method using Fmoc chemistry. The N- and C-termini were each capped with an acetyl group and an amide group, respectively. The peptide molecular masses were determined by matrix-assisted laser desorption ionization mass spectrometry using an Applied Biosystems Voyager-DE PRO (Table 1).

The SAA proteins were freshly dialyzed from 4 M urea into ultrapure water, and the SAA peptides were dissolved in ultrapure water. Protein or peptide solutions were centrifuged to remove any insoluble or aggregated matter before use. The protein solutions were maintained at 4 °C throughout the preparation. Protein or peptide concentrations were determined by the Lowry method, using bovine serum albumin (Bio-Rad, Hercules, CA) as a standard.

Table 1
Amino acid sequences and molecular masses of synthetic fragment peptides.

Peptide	Sequence	Found: *m/z* (calculated: M+H)
SAA1.1 (43–63)	DAAKRGPGGVWAAEAISDARE	2169.2 (2168.1)
SAA1.3 (43–63)	DAAKRGPGGAWAAEAISDARE	2140.5 (2140.1)
SAA1.5 (43–63)	DAAKRGPGGAWAAEVISDARE	2168.4 (2168.1)

2.3. Circular dichroism (CD) spectroscopy

Far-ultraviolet CD spectra were recorded at 4 °C or 37 °C with an Aviv 62ADS spectropolarimeter (Lakewood, NJ). The results were corrected by subtracting the baseline of an appropriate blank sample. The mean residual ellipticity ([θ]) was calculated using the equation $[\theta] = (\mathrm{MRW})\,\theta/10lc$, where θ is the measured ellipticity in degrees, l is the cuvette path length (0.2 cm), c is the protein or peptide concentration in g/mL, and the mean residue weight (MRW) is obtained from the molecular weight and the number of amino acids. The protein or peptide concentrations were 50 μg/mL. For fibril formation experiments, the measurements were performed 1 day after sample preparation.

2.4. Fluorescence spectroscopy

All fluorescence measurements were performed at 4 °C or 37 °C on a Hitachi F-7000 spectrophotometer (Tokyo, Japan). ThT fluorescence spectra were recorded in a 4 × 4 mm cuvette from 450 to 600 nm at an excitation wavelength of 440 nm. The ThT, heparin, and protein or peptide concentrations were 10 μM, 41 μg/mL, and 50 μg/mL, respectively.

2.5. Transmission electron microscopy (TEM)

Samples were applied to carbon-coated copper grids (400-mesh) and negatively stained with 2% (w/v) uranyl acetate. These samples were examined under a JEM-1200EX transmission electron microscope (JEOL, Akishima, Japan) with an acceleration voltage of 80 kV. The observations were performed at least 6 days after sample preparation.

3. Results

3.1. Secondary structure of the SAA1 isoforms

Secondary structures of SAA were analyzed by CD spectroscopy at pH 7.4. Fig. 1 illustrates the typical CD spectra for SAA1.1 at 4 °C and 37 °C. At 37 °C, the CD spectrum showed a single minimum of approximately 200 nm, indicating that the SAA1.1 molecule had formed a random coil structure. In contrast, at 4 °C, the CD spectrum exhibited double minima at approximately 208 and 222 nm, representing the potential propensity of the SAA1.1 molecule to form an α-helical structure. SAA1.1 reversibly formed an α-helical structure at 4 °C, even after measurement at 37 °C. SAA1.3 and SAA1.5 showed similar results, indicating that all SAA1 isoforms adopted α-helix structures at 4 °C, but were unstructured at 37 °C.

3.2. Amyloid fibril formation of the SAA1 isoforms

Amyloid fibril formation of the SAA1 isoforms was investigated using a fluorescent dye (ThT), which is well-known to specifically bind to ordered β-sheet aggregates [14]. Fig. 2A and B illustrate the pH-dependent increase in ThT fluorescence after 1 day of incubation following the addition of heparin to SAA1.1 at 37 °C and 4 °C, respectively. Heparin, an analog of heparan sulfate, has been shown to stimulate the fibril formation of many amyloidogenic polypeptides [15,16]. In the absence of heparin, no ThT fluores-

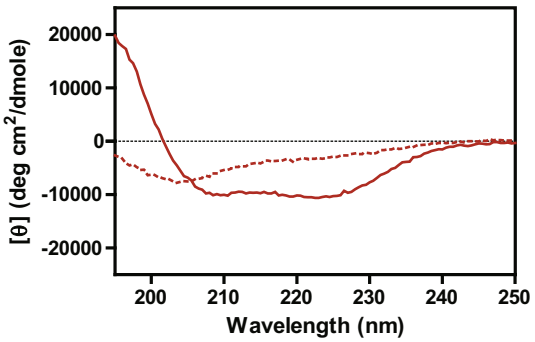

Fig. 1. CD spectra of SAA1.1 at 4 °C (solid line) and 37 °C (dashed line) (pH 7.4).

cence was observed at any of the pH values tested over the course of 6 days (data not shown), consistent with a previous study showing that the fibril formation of SAA peptides was facilitated by the addition of heparin [10]. A significant increase in ThT fluorescence was observed at pH 4.0 and 5.6, but not at pH 7.4, when SAA1.1 was incubated with heparin at both temperatures (Fig. 2A and B).

Fig. 2C and D illustrate the typical CD spectra of SAA1.1 at 37 °C and 4 °C (pH 4.0), respectively, in the absence and presence of heparin. Compared with the results shown in Fig. 1, which was obtained at pH 7.4, no significant differences were observed in the CD spectra for SAA1.1 in the absence of heparin at both temperatures, suggesting that the secondary structure of the SAA1.1 molecule was unaffected by the change in pH. In contrast, remarkable changes were observed in the CD spectrum for SAA1.1 incubated with heparin at 37 °C, showing a single minimum at approximately 220 nm, characteristic of a β-sheet structure (Fig. 2C). On the other hand, despite the significant increase in ThT fluorescence (Fig. 2B), the CD spectrum for SAA1.1 incubated with heparin at 4 °C retained double minima at approximately 208 and 222 nm, which was in sharp contrast to Fig. 2C (Fig. 2D).

We compared the ThT fluorescence and CD spectra of three SAA1 isoforms at 37 °C and 4 °C (pH 4.0). Comparable heparin-induced increases in ThT fluorescence were observed in all the SAA1 isoforms (Fig. 3A and B). Likewise, almost identical CD spectra were obtained in the presence of heparin at each temperature (Fig. 3D and E). ThT fluorescence and CD results demonstrate that all the SAA1 isoforms are postulated to form fibrils at both temperatures, but not typical amyloid fibrils at 4 °C.

3.3. Fibril morphology of the SAA1 isoforms

The morphologies of fibrils formed in the presence of heparin at pH 4.0 and 37 °C were examined by TEM. In an SAA1.1 sample at a concentration of 50 μg/mL, incubated under conditions equivalent to those applied above, a spherical morphology was observed (Fig. 4A) despite the increase in ThT fluorescence and the formation of a β-sheet structure. Similar TEM images were obtained for the SAA1.3 and SAA1.5 samples under the same conditions. When the concentrations of SAA1 samples incubated for fibril formation were raised to 500 μg/mL without changing the heparin concentration, precipitates were detected immediately after the addition of heparin, in contrast to the "regular" condition of 50 μg/mL. No visible aggregates were observed in the TEM images of the supernatants alone, as anticipated from the lack of increase in ThT fluorescence. A dispersion that included the precipitates revealed a noisy spectrum but a pronounced increase in ThT fluorescence. TEM images of the dispersed samples exhibited fibrils that were clearly distinguishable from the spherical morphology; fibrils with curly morphologies were observed in the SAA1.1 sample at a concentration of 900 μg/mL (Fig. 4B), consistent with a previous report

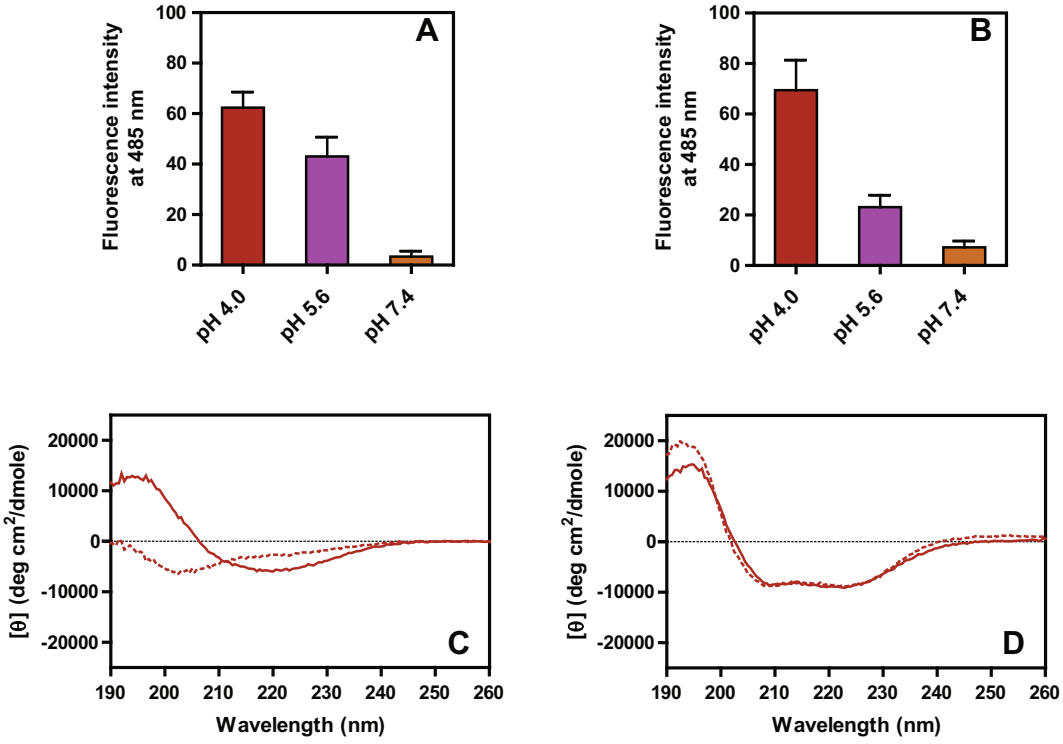

Fig. 2. (A and B) ThT fluorescence intensities at 485 nm of SAA1.1 after incubation with heparin under three different pH conditions (pH 4.0: red, pH 5.6: pink, pH 7.4: orange) at (A) 37 °C and (B) 4 °C. (C and D) CD spectra of SAA1.1 in the absence (dashed line) and presence (solid line) of heparin at (C) 37 °C and (D) 4 °C (pH 4.0). (For interpretation of the references to color in this figure legend, the reader is referred to the web version of this article.)

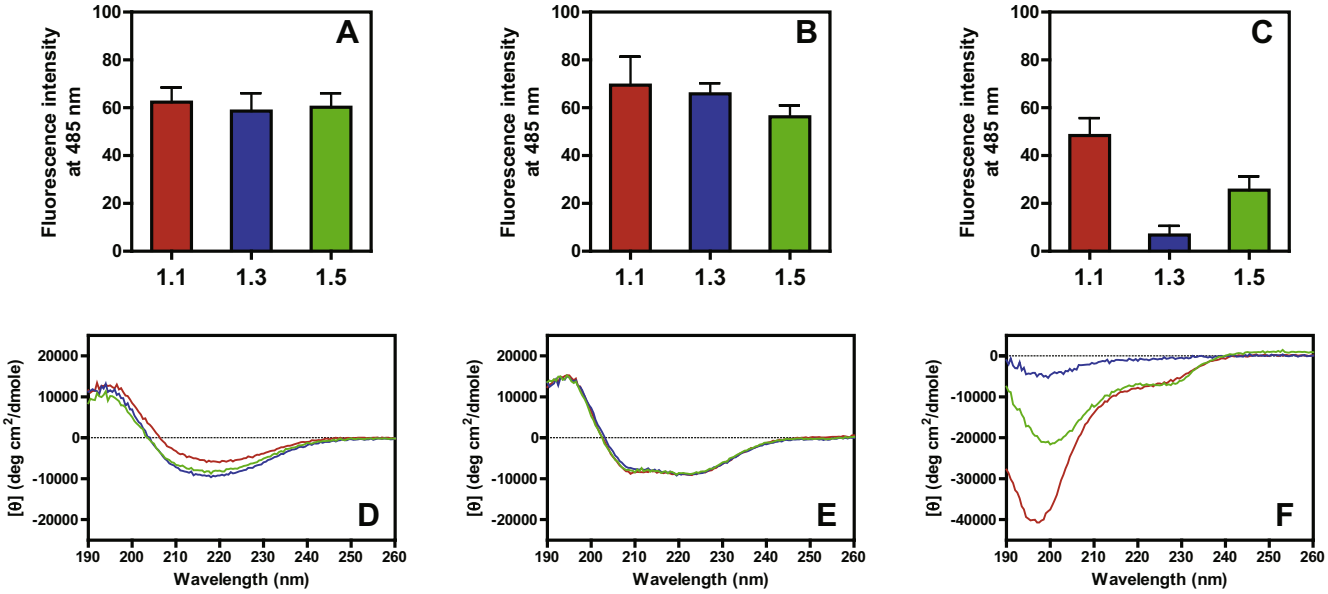

Fig. 3. (A–C) ThT fluorescence intensities at 485 nm of the three SAA1 isoforms (1.1: red, 1.3: blue, 1.5: green) in the presence of heparin (pH 4.0). Full-length proteins at (A) 37 °C and (B) 4 °C. (C) Central peptides at 37 °C. (D–F) CD spectra of the three SAA1 isoforms (1.1: red, 1.3: blue, 1.5: green) in the presence of heparin (pH 4.0). Full-length proteins at (D) 37 °C and (E) 4 °C. (F) Central peptides at 37 °C. (For interpretation of the references to color in this figure legend, the reader is referred to the web version of this article.)

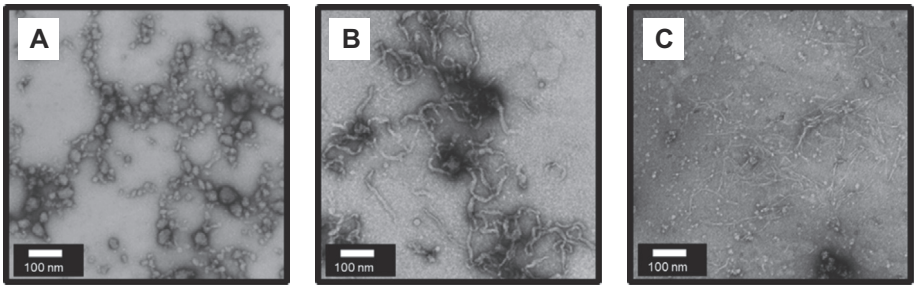

Fig. 4. Transmission electron micrographs of SAA1.1 samples incubated at (A) 50 μg/mL and (B) 900 μg/mL and (C) an SAA1.3 sample incubated at 500 μg/mL.

[12]. In contrast, fibrils with relatively thin and straight morphologies were observed in the SAA1.3 sample at a concentration of 500 μg/mL (Fig. 4C).

3.4. Amyloid fibril formation of SAA peptides

In order to compare the amyloidogenic properties of three SAA1 isoforms in detail, we investigated the amyloid fibril formation of the synthetic fragment peptides that corresponded to the central regions of the SAA1 isoforms at pH 4.0 and 37 °C. The ThT fluorescence intensity of the SAA1.1 (43–63) peptide was consistent with previous results [10]. As shown in Fig. 3C, the SAA1.3 (43–63) peptide showed little increase in ThT fluorescence compared with the SAA1.1 (43–63) peptide, whereas the SAA1.5 (43–63) peptide fluorescence increase fell between those of the others.

Fig. 3F illustrates the typical CD spectra of the three SAA (43–63) peptides that were incubated with heparin at pH 4.0. These peptides formed random coil structures in the absence of heparin. No spectral changes in the SAA1.3 (43–63) peptide were observed by the addition of heparin. Although the magnitude of the SAA1.5 (43–63) peptide was smaller than that of the SAA1.1 (43–63) peptide, both the SAA1.1 and 1.5 (43–63) peptides showed a large minimum of approximately 200 nm, together with a slight shoulder around 220 nm after the addition of heparin, suggesting the possible coexistence of a β-sheet structure. Taken together with the results of ThT fluorescence, it is plausible that the central regions of the human SAA1 isoforms have distinct amyloidogenic properties, despite having only a single amino acid variation at two sites.

4. Discussion

4.1. Disparities between the full-length protein and the fragment peptide

As shown in Fig. 2A and B, SAA fibril formation in response to the addition of heparin was accelerated under more acidic conditions. The SAA1.1 (43–63) peptide formed fibrils only at pH 4.0 in the previous study [10], whereas the SAA1.1 protein showed an enhancement in ThT fluorescence not only at pH 4.0 but also at pH 5.6. Taking the predicted isoelectric points (p*I*) of these molecules (SAA1.1 protein; p*I* = 5.9 and SAA1.1 (43–63) peptide; p*I* = 4.8) into account, the p*I* values appear to correlate with the occurrence of fibril formation. These results were obtained most likely because electrostatic interactions between negatively charged heparin, with a large number of sulfate groups, and positively charged SAA molecules under acidic conditions (lower than the p*I*) would be strengthened. In fact, even at pH 4.0, fibril formation was inhibited in the presence of 0.15 M NaCl.

Although there were almost no differences in the propensities of fibril formation among the full-length SAA1 isoforms, the SAA central region peptides had varied abilities to form fibrils, with the SAA1.3 (43–63) peptide being the least amyloidogenic. One possible explanation for the peptide results is that each amino acid has a distinct propensity to form secondary structures. At the mutation sites, the SAA1.1 and 1.5 molecules have one Ala and one Val residue, whereas the SAA1.3 molecule has two Ala residues, which are less prone to form a β-sheet structure than Val [17].

C-terminal region truncation is crucial to the pathogenesis of AA amyloidosis [18]. Although the SAA C-terminal region does not directly contribute to amyloid fibril formation [10], the presence of the C-terminal region in the full-length protein could hamper the binding of other regions to heparin because heparin/heparan sulfate binding occurs through the C-terminal region [19]. Thus, it is also possible that the C-terminal regions in the full-length SAA1 isoforms conceal the differences in amyloidogenic propensities observed in the fragment peptides with amino acid variations. Further studies with C-terminal region-truncated polypeptides (such as AA fragment) are required to verify such possibilities. At present, we unsuccessfully attempted to produce a C-terminal truncated protein in an *E. coli* expression system, probably because the mRNA and/or product protein stability is quite low.

4.2. Unexpected detection of ThT fluorescence with SAA aggregates

Although the mode of binding of ThT to amyloid fibrils is under debate, ThT has been postulated to recognize amyloid fibril β-sheet structures [20]. However, a significant increase in ThT fluorescence was observed, although the CD spectra for the SAA1 isoforms in the presence of heparin indicated α-helical structures at pH 4.0 and 4 °C (Fig. 3B and E). These results cannot rule out the possibility that the SAA1 isoforms contain β-sheet structures because CD spectroscopy is less sensitive to β-sheet structures [21]. Within the SAA1 molecule, which intrinsically forms an α-helical structure at 4 °C, regions unnecessary for fibril formation are assumed to retain α-helical structures even after an incubation with heparin. Consequently, CD signals derived from β-sheet structures may be disregarded because of the spectral overlap with those from α-helical structures. Thus, detailed structural analyses that incorporate modalities such as infrared spectroscopy are required to comprehensively address this issue [21]. However, these would be technically difficult because CD measurements revealed that the α-helical fibrils that formed at 4 °C converted to β-sheet structures immediately after the temperature was increased to 37 °C (data not shown). Similarly, the CD spectra for the SAA1.1 and SAA1.5 (43–63) peptides were not typical of β-sheet structures, despite a significant increase in ThT fluorescence (Fig. 3C and F). Noting a slight shoulder at approximately 220 nm, it is feasible that these peptides form partial β-sheet structures. Accordingly, as postulated for most amyloid fibrils, ThT is assumed to bind only to the β-sheet region involved in SAA molecule fibril formation.

4.3. Spherical aggregates as a possible intermediate structure for amyloid fibril formation

TEM images of SAA1.1 proteins at 50 μg/mL showed spherical structures, despite possessing certain typical features of amyloid fibrils (Figs. 2A, C, and 4A). Spherical structures were also observed in the aggregates of amyloid-β (1–40) peptide, in which fibrillar structures became the dominant species in an incubation time-dependent manner [22]. The initial concentration is proposed to be a crucial factor for the formation of α-synuclein amyloid fibrils, in which fibrillar structures became the dominant species above the initial threshold concentration [23]. Given the observation that fibrillar structures were observed in SAA1 samples at higher protein concentrations, SAA is considered to form amyloid fibrils through spherical intermediates. The protein concentration and/or the incubation time required to form mature fibrils may be insufficient in the current experimental conditions with the SAA1.1 proteins. Spherical aggregates of soluble oligomers were recently demonstrated in human SAA1.1 molecules during the early stages of the amyloid formation pathway [24].

4.4. Relevance of the SAA1 isoforms in the pathogenesis of AA amyloidosis

In the previous study, the N-terminal (1–27) peptide common to the three SAA1 isoforms formed short and straight fibrils, which is typical of amyloid fibrils, whereas the SAA1.1 (43–63) peptide formed long and seemingly elastic fibrils [10]. Accordingly, the involvement of both the central region and the N-terminal region of the SAA1.1 molecule could lead to the formation of flexible fibrils. In contrast, the SAA1.3 (43–63) peptide showed little increase in ThT fluorescence and no conformational changes, suggesting that the central region of the SAA1.3 molecule is supposed to be non-amyloidogenic. Thus, the fibril morphology observed with the SAA1.3 molecule was similar to that observed with the N-terminal peptide. It is possible that the amyloidogenic propensities of the SAA molecule central region affect the fibril morphology of the full-length protein.

Although the frequencies of the three SAA1 isoforms are nearly equal in a normal population, rheumatoid arthritis patients with the SAA1.3 isoform have the highest risk of AA amyloidosis, followed by those with the SAA1.5 and 1.1 isoforms in Japanese populations [9]. That is, the prevalence of AA amyloidosis can be influenced by the SAA1 isoforms. Fibril morphology can affect cytotoxicity. For example, insulin fibrils with a typical straight morphology are more cytotoxic than curly fibrils [25]. It is conceivable that differences in fibril morphology among the SAA1 isoforms would affect the pathogenesis of AA amyloidosis, such that involvement of the SAA1.1 molecule central region in amyloid fibrils would inhibit the formation of highly cytotoxic fibrils by forming curly fibrils. However, because amyloid fibril formation is caused not only by the amyloidogenic propensities of proteins but also by the complex interactions with disease-modifying factors, a comprehensive and detailed understanding of the underlying molecular mechanism is required to elucidate the pathogenesis of AA amyloidosis.

In the present study, we revealed that human SAA1 was unstructured at a physiological temperature. Moreover, we demonstrated that human SAA1 formed amyloid fibrils in the presence of heparin. Although there was almost no difference in the heparin-induced amyloid fibril formation of the three SAA1 isoforms, the central peptides that corresponded to each SAA1 isoform showed distinct amyloidogenic properties. These results raise the possibility that amino acid variations in the SAA1 molecule central region could directly affect amyloid fibril formation, particularly fibril morphology, and may influence the prevalence of AA amyloidosis.

Acknowledgments

We are indebted to Dr. Satomi Nadanaka (Department of Biochemistry, Kobe Pharmaceutical University) for her valuable advice. This study was supported in part by a Grant from the Strategic Research Foundation Grant-aided Project for Private Universities from the Ministry of Education, Culture, Sport, Science, and Technology, Japan, 2012–2017 (S1201040) and a Grant to the Amyloidosis Research Committee for Research on Intractable Diseases from the Ministry of Health, Labor and Welfare, Japan.

References

[1] J.D. Gillmore, L.B. Lovat, M.R. Persey, M.B. Pepys, P.N. Hawkins, Amyloid load and clinical outcome in AA amyloidosis in relation to circulating concentration of serum amyloid A protein, Lancet 358 (2001) 24–29.

[2] F.C. De Beer, R.K. Mallya, E.A. Fagan, J.G. Lanham, G.R. Hughes, M.B. Pepys, Serum amyloid-A protein concentration in inflammatory diseases and its relationship to the incidence of reactive systemic amyloidosis, Lancet 2 (1982) 231–234.

[3] L. Obici, G. Merlini, AA amyloidosis: basic knowledge, unmet needs and future treatments, Swiss Med. Wkly. 142 (2012) w13580.

[4] C.M. Uhlar, A.S. Whitehead, Serum amyloid A, the major vertebrate acute-phase reactant, Eur. J. Biochem. 265 (1999) 501–523.

[5] X. Zhang, J.P. Li, Heparan sulfate proteoglycans in amyloidosis, Prog. Mol. Biol. Transl. Sci. 93 (2010) 309–334.

[6] J.N. Buxbaum, R.P. Linke, A molecular history of the amyloidoses, J. Mol. Biol. 421 (2012) 142–159.

[7] M. Fandrich, Oligomeric intermediates in amyloid formation: structure determination and mechanisms of toxicity, J. Mol. Biol. 421 (2012) 427–440.

[8] H. LeVine 3rd, Thioflavine T interaction with synthetic Alzheimer's disease beta-amyloid peptides: detection of amyloid aggregation in solution, Protein Sci. 2 (1993) 404–410.

[9] T. Yamada, Y. Okuda, K. Takasugi, L. Wang, D. Marks, M.D. Benson, B. Kluve-Beckerman, An allele of serum amyloid A1 associated with amyloidosis in both Japanese and Caucasians, Amyloid 10 (2003) 7–11.

[10] M. Egashira, H. Takase, I. Yamamoto, M. Tanaka, H. Saito, Identification of regions responsible for heparin-induced amyloidogenesis of human serum amyloid A using its fragment peptides, Arch. Biochem. Biophys. 511 (2011) 101–106.

[11] T. Yamada, A. Wada, Slower clearance of human SAA1.5 in mice: implications for allele specific variation of SAA concentration in human, Amyloid 10 (2003) 147–150.

[12] T. Yamada, B. Kluve-Beckerman, J.J. Liepnieks, M.D. Benson, Fibril formation from recombinant human serum amyloid A, Biochim. Biophys. Acta 1226 (1994) 323–329.

[13] S. Ohta, M. Tanaka, K. Sakakura, T. Kawakami, S. Aimoto, H. Saito, Defining lipid-binding regions of human serum amyloid A using its fragment peptides, Chem. Phys. Lipids 162 (2009) 62–68.

[14] M. Biancalana, S. Koide, Molecular mechanism of thioflavin-T binding to amyloid fibrils, Biochim. Biophys. Acta 2010 (1804) 1405–1412.

[15] F. Noborn, P. O'Callaghan, E. Hermansson, X. Zhang, J.B. Ancsin, A.M. Damas, I. Dacklin, J. Presto, J. Johansson, M.J. Saraiva, E. Lundgren, R. Kisilevsky, P. Westermark, J.P. Li, Heparan sulfate/heparin promotes transthyretin fibrillization through selective binding to a basic motif in the protein, Proc. Natl. Acad. Sci. USA 108 (2011) 5584–5589.

[16] S. Jha, S.M. Patil, J. Gibson, C.E. Nelson, N.N. Alder, A.T. Alexandrescu, Mechanism of amylin fibrillization enhancement by heparin, J. Biol. Chem. 286 (2011) 22894–22904.

[17] P.Y. Chou, G.D. Fasman, Prediction of protein conformation, Biochemistry 13 (1974) 222–245.

[18] T. Yamada, N. Hirano, T. Kuroda, Y. Okuda, Y. Itoh, Generation and characterization of rat monoclonal antibodies against human serum amyloid A, Scand. J. Immunol. 46 (1997) 175–179.

[19] J.B. Ancsin, R. Kisilevsky, The heparin/heparan sulfate-binding site on apo-serum amyloid A. Implications for the therapeutic intervention of amyloidosis, J. Biol. Chem. 274 (1999) 7172–7181.

[20] R. Sabate, L. Rodriguez-Santiago, M. Sodupe, S.J. Saupe, S. Ventura, Thioflavin-T excimer formation upon interaction with amyloid fibers, Chem. Commun. (Camb.) 49 (2013) 5745–5747.

[21] H. Hiramatsu, T. Kitagawa, FT-IR approaches on amyloid fibril structure, Biochim. Biophys. Acta 1753 (2005) 100–107.

[22] S. Chimon, M.A. Shaibat, C.R. Jones, D.C. Calero, B. Aizezi, Y. Ishii, Evidence of fibril-like beta-sheet structures in a neurotoxic amyloid intermediate of Alzheimer's beta-amyloid, Nat. Struct. Mol. Biol. 14 (2007) 1157–1164.

[23] M.E. van Raaij, J. van Gestel, I.M. Segers-Nolten, S.W. de Leeuw, V. Subramaniam, Concentration dependence of alpha-synuclein fibril length assessed by quantitative atomic force microscopy and statistical–mechanical theory, Biophys. J. 95 (2008) 4871–4878.

[24] S. Patke, S. Srinivasan, R. Maheshwari, S.K. Srivastava, J.J. Aguilera, W. Colon, R.S. Kane, Characterization of the oligomerization and aggregation of human serum amyloid A, PLoS One 8 (2013) e64974.

[25] T. Zako, M. Sakono, N. Hashimoto, M. Ihara, M. Maeda, Bovine insulin filaments induced by reducing disulfide bonds show a different morphology, secondary structure, and cell toxicity from intact insulin amyloid fibrils, Biophys. J. 96 (2009) 3331–3340.